Neuroradiology (1992) 34: 413–416

Neuro radiology

Magnetic resonance imaging and angiography in hemifacial spasm

S. Felber[1], G. Birbamer[1], F. Aichner[1], W. Poewe[3], and A. Kampfl[2]

Departments of [1] Magnetic Resonance and [2] Neurology, University of Innsbruck, Austria
[3] Department of Neurology, University of Berlin, Federal Republic of Germany

Received: 22 January 1992

Summary. We used magnetic resonance imaging (MRI) and magnetic resonance angiography (MRA) to investigate 14 patients with unilateral hemifacial spasm (HS) and 20 controls. The relationship of the seventh and eighth cranial nerves to adjacent vessels was best visualized on the contiguous flow sensitive 3D-FISP images. Reconstruction of projectional MRA was helpful to assess the complex architecture of the vertebrobasilar system. Neurovascular contact in the facial nerve root exit zone was present in 4 of 20 controls and in 12 of 14 patients, in whom it predicted the affected side. These results support previous findings of surgical and electrophysiological investigations that local irriation of the facial nerve is the most possible explanation for HS. MRI and MRA provide vascular and brain tissue diagnosis in a single non-invasive examination and should be recommended as primary neuroradiological procedure in HS.

Key words: Cerebral blood vessels – Hemifacial spasm – Magnetic resonance imaging – Magnetic resonance angiography

Hemifacial spasm (HS) is a disease of middle and later life, characterized by involuntary, paroxysmal, painless contractions of the muscles innervated by the seventh cranial nerve [1]. It is rarely (< 2%) caused by tumours, aneurysms or arteriovenous malformations in the cerebellopontine angle [2–4]. In the majority of cases there is no evidence of a structural lesion and HS in the past was considered idiopathic [5]. Based on surgical findings it is now widely accepted that compression of the facial nerve near its root exit zone (REZ) on the caudal brain stem by loops of otherwise normal-appearing vessels is the most frequent cause. The vertebral (VA), posterior cerebellar (PICA) or anterior cerebellar arteries (AICA) and less commonly the cochlear or basilar arteries (BA) or veins have been described as responsible for HS [6–8]. CT has been effective in delineation of tortuous, ectatic, dilated vascular channel crossing the brain stem from one cerebellopontine angle to the other side [9]. CT and X-ray angiography were used in the diagnosis of HS, primarily to exclude posterior fossa tumours and vascular malformations. Routine CT techniques are inadequate to delineate the facial nerve in relation to smaller vessels and X-ray angiography does not visualize neural structures [10–12].

Recent reports have emphasized the potential of conventional magnetic resonance (MR) techniques for demonstration of neurovascular contact in HS and in trigeminal neuralgia [13–15].

We introduced a high-resolution, non-invasive MR angiography (MRA) protocol into routine HS diagnosis to evaluate the potential of combined MR imaging (MRI) and MRA in diagnosis of HS.

Methods

Between May 1988 and December 1989, 14 patients with unilateral HS entered a combined MRI/MRA study. All had "essential" HS, documented by neurological examination, absence of posterior cranial fossa masses on CT and follow-up for at least 2 years. There were 8 women and 6 men, aged 46–69 years (mean 57 years). Duration of the disease ranged from 2 to 22 years with a mean of 7.3 years.

Table 1. MRI and MRA findings in 14 patients with unilateral hemifacial spasm (HS)

Age/sex	HS side/duration (years)	Tortuosity of VA/BA (side of convexity)	NVC/REZ
52/m	L (4.5)	VA (L)/BA (R)	VA (L)
58/m	L (4.0)	VA (L)/BA (R)	VA (L)
55/m	L (3.5)	VA (L)/BA (R)	VA (L)
64/f	L (11)	VA (L)/BA (R)	VA (L)
62/f	L (9.0)	VA (L)	VA (L)
46/f	L (2.0)	VA (L)/BA (R)	PICA (L)
59/f	R (9.0)	VA (R)/BA (L)	PICA (R)
69/f	L (8.5)	VA (L)	PICA (L)
48/m	L (4.0)	VA (L)	PICA (L)
67/f	R (12)	VA (L)/BA (R)	AICA (R)
59/m	R (2.0)	Normal	PICA (R)
59/f	L (22)	Normal	PICA (L)
52/m	R (4.5)	Normal	Normal
49/f	R (6.0)	Normal	Normal

NVC, Neurovascular contact; REZ, root exit zone; VA, vertebral artery; BA, basilar artery; f, female; m, male; R, right; L, Left

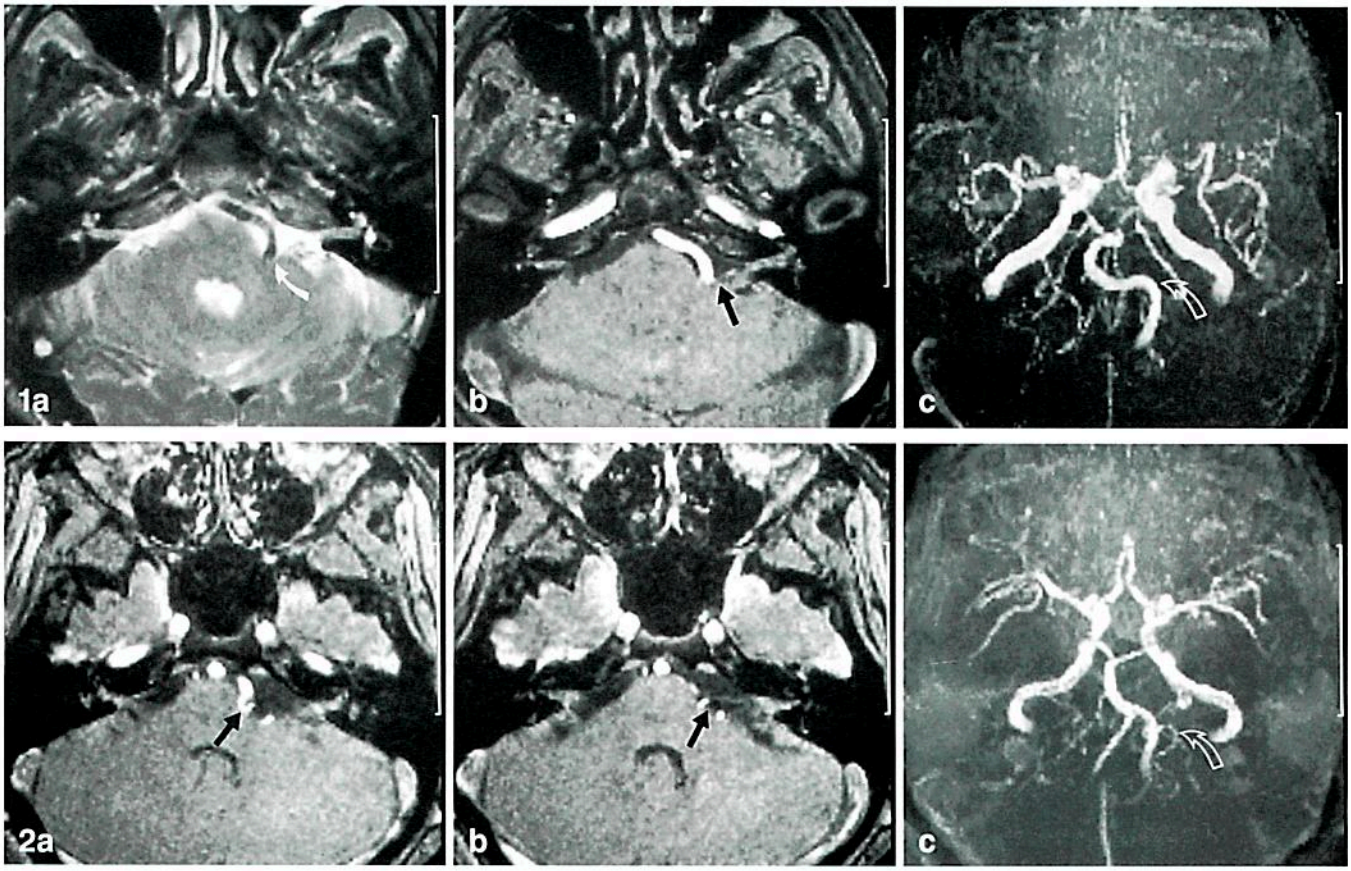

Fig. 1 a–c. A 58-year-old patient, left hemifacial spasm (HS) for 4 years. **a** T2-weighted image shows the vertebral artery (VA) extending into the left cerebellopontine angle, compressing the brain stem and the facial nerve root exit zone (REZ) *(arrow)*. **b** Representative 1.1 mm slice of the 3D-FISP acquisition at same level displays the VA with high signal intensity and better delineates the displaced facial nerve on the left *(arrow)*. **c** Projectional magnetic resonance angiography (MAR), viewed 45° from below in an anteroposterior direction (calculated from the 3D-FISP 88 images in **b**) shows tortuous elongation of the VA and basilar artery (BA) with left and right convexity respectively. Note also non-visualization of the right VA

Fig. 2 a–c. A 69-year-old patient, with left HS for 8.5 years. **a,b** Adjacent 1.1 mm slices of the 3D-FISP acquisition. A loop of the posterior inferior cerebellar artery (PICA) is pushed upwards between the seventh and eighth cranial nerves, indenting the REZ of the facial nerve from below (**b**). Its origin from the VA is demonstrated in **a** *(arrow)*. **c** The reconstructed MRA, viewed 60° from below, shows opposite convexity of the VA and BA as well as the cranial loop of the PICA on the left side *(arrow)*

In 5 cases HS affected the right facial muscles and in 9 the left. Informed consent was obtained in all patients.

The MR investigations were performed on a 1.5 T unit, equipped with a 10 mT gradient system using a circular polarized, transmit/receive head coil (FOV = 23 cm). The examination protocol consisted of sagittal T1-weighted (TR = 500/TE = 15/NEX = 2) and transverse long TR short and long TE (TR = 2400/TE = 15,90/NEX = 1) multislice spin-echo (SE) sequences with 5-mm slice thickness. A 3D-FISP sequence was used for MRA in transverse orientation to provide inflow enhancement of unsaturated spins. Motion-induced signal loss due to phase effects was compensated by refocussing gradients for constant velocities in slice-select and read-out direction. Small FOV (20–23 cm) and short TE (7 ms) minimized intravoxel phase dispersion related to higher order motion and susceptibility effects. Sequence parameters had been empirically adjusted to maximize contrast between moving blood and stationary tissue (TR = 40 ms, 15°). The excitation volume (6.4–7 cm) was divided by 64 phase-encoding steps into contiguous, 1- to 1.2-mm slices. The individual MRA images (Figs. 2b, 3a,b, 4a,b, 5a,b) were postprocessed by a previously described ray-tracer algorithm [16] to projectional MRA (Fig. 2c). We calculated 36 projections at 10° increments in the x and y axes [17–21]. The MRI and MRA were assessed for the presence of intracranial abnormalities, visualization of the VII cranial nerve and vessels indenting the REZ of the facial nerves by two of us (S.F., G.B.) blinded to the symptomatic side. The REZ was anatomically defined as the central and anterior portion of the facial nerve. In addition, the MRA of 20 patients suffering from arteriosclerotic disease (49–75 years of age), without evidence of HS, were reviewed for neurovascular contact at the facial nerve REZ.

Table 2. MRI and MRA findings of neurovascular contact at the root exit zone in 14 patients with unilateral HS

Neurovascular contact	MRI T1/T2 SE sequences	MRA 3D-FISP
Tortuous VA	8	5
Branches pushed up against the REZ by a tortuous VA or BA		
PICA	1	4
AICA		1
PICA loop	1	2
Normal	4	2

BA, Basilar artery; VA, vertebral artery; REZ, root exit zone; AICA, PICA anterior and posterior inferior cerebellar arteries

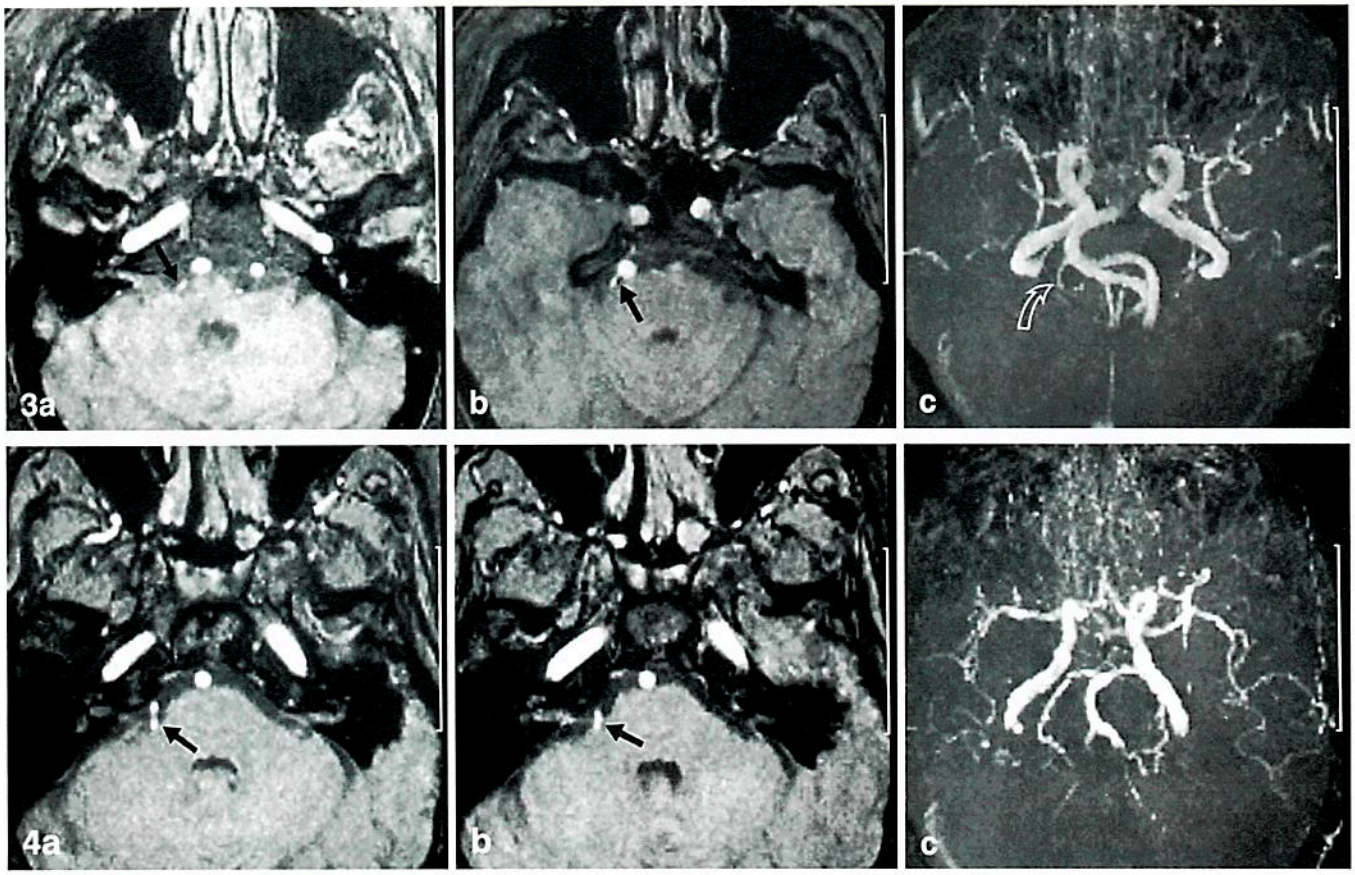

Fig. 3a–c. A 67-year-old patient, HS on the right for 12 years. **a, b** Two representative 1 mm slices of the 3D-FISP sequence. The REZ of the right facial nerve is indented by the anterior inferior cerebellar artery (AICA) *(arrow in a)*, seen originating from the BA *(arrow in b)*. **c** The reconstructed projection (45° from above) MRA confirms the extensive elongation of the VA and BA. The origin of the symptomatic AICA is better demonstrated than on the 2D-cross-sections *(arrow)*

Fig. 4a–c. A 59-year-old patient with a 2-year history of right HS. **a, b** Adjacent 3D-FISP 1.2 mm slices show the BA in the midline. There is indentation of the right facial nerve REZ by a cranial loop of the right PICA *(arrows)*. **c** Reconstructed MRA, projected 55° from below, shows the normal course of the BA but fails to demonstrate the right PICA

Results

All MRI/MRA examinations were of diagnostic quality. There were no posterior cranial fossa masses, brain stem abnormalities or lesions within the corticobulbar tracts. The common course of the seventh and eighth cranial nerves from the lower brain stem to the internal auditory canal was seen best on 3D-FISP images. The vertebrobasilar system of 10 of the 14 patients showed tortuous elongation, demonstrated equally on SE and MRA images. All elongated VAs extended into the cerebellopontine angle; in 9 of the 10 cases the convexity pointed to the symptomatic facial nerve. Contralateral convexity of the BA was present in 7 of these 10 patients but only one convex BA was directed towards the symptomatic facial nerve.

Vessels crossing the REZ of the facial nerve were noted by both readers in 10 of 14 SE studies and 12 of 14 MRA examinations (Table 1). Neurovascular contact was always on the side affected by HS. No patient had evidence of neurovascular contact at the REZ on the asymptomatic side. Four of 20 age-matched controls without HS had vessels crossing the facial nerve REZ.

Contact between the REZ and an elongated VA and/or displaced branches was found in 10 patients. MRA was significantly more precise than MRI (Table 2) in differentiating direct neurovascular contact by the VA (Fig. 1) from branches pushed up against the REZ by a tortuous VA (Figs. 2, 3). In 2 patients neurovascular contact was caused by a prominent loop of an anatomically dominant PICA (Fig. 4).

Discussion

The results of microsurgical neurovascular decompression, supported by electrophysiological data, indicate that contact between the facial nerve REZ and vascular structures is the most likely cause of "essential" HS [1, 22]. Continuous or pulsatile compression is thought to cause focal demyelination at the junction between central and peripheral myelin (REZ) leading to increased neuronal discharge in the facial nucleus via ephaptic transmission and/or antidromic stimulation [23]. However, in some patients, surgery remains exploratory and recent reports of HS caused by nuclear and supranuclear parenchymal lesions underline that more than one anatomical location may be involved in pathogenesis [24, 25].

The advantages of MRI in the investigation of the cranial nerves and their relationship to adjacent vessels have already been recognized [14, 15]. Routinely applied 2D-SE-sequence techniques show vascular structures as dark, due to time-of-flight effects, which limits the differentiation of smaller vessels from CSF or brain parenchyma. The results of our prospective study demonstrate that sensitivity towards small vessels could be significantly improved by the use of high-resolution 3D-MRA sequences.

Neurovascular contact was observed on MRA in 86% and on SE images in 71% of patients. In addition, the vessel responsible for neurovascular contact was delineated more precisely on MRA. On 3 occasions SE images showed a redundant VA, but MRA changed the diagnosis into a dislocated PICA, pushed towards the REZ.

Of 46 HS patients studied by CT 36 had dolichovertebrobasilar arteries whose convexity was on the side of the spasms in 92% [26]. In our series convexity of the VA had high correlation with clinical lateralization, whereas convexity of the BA correctly indicated the symptomatic side in only 1 patient. Differentiation of neurovascular contact due to the vertebrobasilar artery or to dislocated branches was superior on high-resolution 3D-FISP images, which also showed looping branches of a normal VA or BA. Anatomical factors such as a dominant PICA or AICA can be responsible for the occurrence HS [11].

Flow-sensitive FISP images were more informative than projectional MRA. Some of the fine vascular details lost by the ray-tracing algorithm were adequately depicted by the original 3D-FISP images (Fig. 4).

Like conventional X-ray angiography, projectional MRA selectively displays vascular structures and is therefore not capable of showing the relationship of vessels to neural tissue. This explains why X-ray angiography is reported as normal in most cases of "essential" HS [11]. Since MRA is calculated from individual cross-sectional images, this technique combines the advantages of both parenchymal diagnosis and projectional angiograms.

Vascular enhancement occurred primarily in arteries. The spatial resolution of $0.8 \times 0.8 \times 1$–1.2 mm restricted visualization of smaller branches, and explains negative results in 2 patients.

Positive neurovascular contact on MRA was on the affected side in all 12 patients. None had evidence of vessels crossing the contralateral REZ or other lesions within the facial nucleus or supranuclear pathways. This supports the assumption that pulsatile compression is a major pathophysiological mechanism for HS. However, presence of neurovascular contact is not specific for HS: 4 of 20 control patients suffering from arteriosclerotic disease and vertebrobasilar ischaemia, without HS, showed neurovascular contact at the facial nerve REZ. Little information exists about the time necessary for pulsatile compression to produce HS and asymptomatic neurovascular contact therefore may represent a "pre-HS" state.

Since more than one locus may be involved in the pathogenesis of HS [1] therapeutic decisions require diagnosis of morphology as well as vascular structures. We suggest that a non-invasive diagnostic approach by a combined MRI/MRA protocol improves our understanding of pathophysiological mechanisms leading to HS.

References

1. Digre KB, Corbett JJ (1988) Hemifacial spasm: differential diagnosis, mechanism, and treatment. In: Jankovic J, Tolosa E (eds) Advances in neurology, vol 49. Facial dyskinesias. Raven Press, New York, pp 131–176
2. Sprik C, Wirtschafter JD (1988) Hemifacial spasm due to intracranial tumor, an international survey of botulinum toxin investigators. Ophthalmology 95: 1042–1045
3. Levine DA, Dyck P (1983) Symptomatic hemifacial spasm: case report and review of the literature. Bull Clin Neurosci 48: 139–147
4. Silber MH, Sandok BA, Earnest F (1987) Vascular malformations of the posterior fossa, clinical and radiological features. Arch Neurol 44: 965–969
5. Ehni G, Woltman HW (1945) Hemifacial spasm. Arch Neurol Psychiatry 53: 205–211
6. Janetta PJ, Abbasy M, Maroon JC, Ramos FM, Albin MS (1977) Etiology and definitive microsurgical treatment of hemifacial spasm. Operative techniques and results in 47 patients. J Neurosurg 47: 321–328
7. Loeser JD, Chen J (1983) Hemifacial spasm: treatment by microsurgical facial nerve decompression. Neurosurgery 13: 141–146
8. Auger RG, Piepgras DG, Laws ER (1986) Hemifacial spasm: results of microvascular decompression of the facial nerve in 54 patients. Mayo Clin Proc 61: 640–644
9. Moseley IF, Holland IM (1979) Ectasia of the basilar artery: the breadth of the clinical spectrum and the diagnostic value of computed tomography. Neuroradiology 18: 83–91
10. Sobel D, Norman D, Yorke CH, Newton TH (1980) Radiography of trigeminal neuralgia and hemifacial spasm. AJR 135: 93–95
11. Carlos R, Fukui M, Hasuo K, et al (1986) Radiological analysis of hemifacial spasm with special reference to angiographic manifestations. Neuroradiology 28: 288–295
12. Takamiya Y, Toya S, Kawase T, Takenaka N, Shiga H (1985) Trigeminal neuralgia and hemifacial spasm caused by a tortuous vertebrobasilar system. Surg Neurol 24: 559–562
13. Tash RR, Kier EL, Chyatte D (1988) Hemifacial spasm caused by a tortuous vertebral artery: MR demonstration. J Comput Assist Tomogr 12: 492–494
14. Tash RR, Sze G, Leslie DR (1989) Trigeminal neuralgia: MR imaging features. Radiology 172: 767–770
15. Tash R, Demerrit J, Sze G, Leslie D (1991) Hemifacial spasm: MR imaging features. AJNR 12: 839–842
16. Laub GA, Kaiser WA (1986) MR-angiography with gradient motion refocussing. J Comput Assist Tomogr 12: 377–382
17. Felber SR, Ruggieri PM, Laub GA, Aichner F (1988) MR angiography: application to carotid atherosclerotic disease. Magn Res Imaging 6 [Suppl 1]: 46
18. Ruggieri PM, Laub GA, Masaryk TJ, Modic MT (1989) Intracranial circulation: pulse sequence considerations in three dimensional (volume) MR angiography. Radiology 171: 785–791
19. Masaryk TJ, Modic MT, Ross JS, et al (1989) Intracranial circulation: preliminary clinical results with three-dimensional (volume) MR-angiography. Radiology 171: 793–799
20. Wagle WA, Dumoulin CL, Souza SP, Cline HE (1989) 3DFT MR angiography of carotid and basilar arteries. AJNR 10: 911–919
21. Felber S, Aichner F, Willeit J, Laub G (1989) Three dimensional magnetic resonance angiography: a new noninvasive approach in the assessment of neurovascular disease. J Cereb Blood Flow Metab 9 [Suppl 1]: 362
22. Janetta PJ (1981) Hemifacial spasm. In: Samii M, Janetta PJ eds. The cranial nerves: anatomy, pathology, pathophysiology, diagnosis and treatment. Springer, New York Berlin Heidelberg, pp 484–493
23. Nielsen VK (1984) Pathophysiology of hemifacial spasm. I. Ephaptic transmission and ectopic excitation. Neurology 34: 418–426
24. Ambrosetto P, Forlani S (1988) Lacunar pontine infarction presenting as isolated facial spasm. Stroke 19: 784–785
25. Toda T, Matsumara K (1989) Facial spasm from lacunar infarction of the thalamic ventrolateral nucleus. Stroke 20: 1289–1290
26. Digre KB, Corbett JJ, Smoker WR, McKusker S (1988) CT and hemifacial spasm. Neurology 38: 1111–1113